



Load validation of aero-elastic simulations with measurements performed on a 850kW horizontal-axis wind turbine

Paulsen, U S; Gomiero, M; Larsen, Torben J.; Benini, E.

Published in:
Journal of Physics: Conference Series

Link to article, DOI:
[10.1088/1742-6596/1037/6/062023](https://doi.org/10.1088/1742-6596/1037/6/062023)

Publication date:
2018

Document Version
Publisher's PDF, also known as Version of record

[Link back to DTU Orbit](#)

Citation (APA):
Paulsen, U. S., Gomiero, M., Larsen, T. J., & Benini, E. (2018). Load validation of aero-elastic simulations with measurements performed on a 850kW horizontal-axis wind turbine. *Journal of Physics: Conference Series*, 1037(6), [062023]. <https://doi.org/10.1088/1742-6596/1037/6/062023>

General rights

Copyright and moral rights for the publications made accessible in the public portal are retained by the authors and/or other copyright owners and it is a condition of accessing publications that users recognise and abide by the legal requirements associated with these rights.

- Users may download and print one copy of any publication from the public portal for the purpose of private study or research.
- You may not further distribute the material or use it for any profit-making activity or commercial gain
- You may freely distribute the URL identifying the publication in the public portal

If you believe that this document breaches copyright please contact us providing details, and we will remove access to the work immediately and investigate your claim.

PAPER • OPEN ACCESS

Load validation of aero-elastic simulations with measurements performed on a 850kW horizontal-axis wind turbine

To cite this article: U S Paulsen *et al* 2018 *J. Phys.: Conf. Ser.* **1037** 062023

View the [article online](#) for updates and enhancements.

Related content

- [Comparison of Aero-Elastic Simulations and Measurements Performed on NENUPHAR's 600kW Vertical Axis Wind Turbine: Impact of the Aerodynamic Modelling Methods](#)
F. Blondel, C. Galinos, U. Paulsen et al.
- [Investigation of the complete power conversion chain for small vertical- and horizontal-axis wind turbines in turbulent winds](#)
M Duponcheel, C Leroi, S Zeoli et al.
- [Analysis of winglets and sweep on wind turbine blades using a lifting line vortex particle method in complex inflow conditions](#)
Matias Sessarego, Néstor Ramos-García and Wen Zhong Shen

Load validation of aero-elastic simulations with measurements performed on a 850kW horizontal-axis wind turbine

U S Paulsen², M Gomiero¹, T J Larsen² and E Benini¹

¹Department of Industrial Engineering, University of Padua, Veneto, Italy.

²Wind Energy Department, Technical University of Denmark, DK 4000 Roskilde Denmark.

E-mail: uwpa@dtu.dk

Abstract. In this work, aero-elastic solver predictions with HAWC2 are compared with measured data from a VESTAS V52 wind turbine situated at DTU campus Risø. Nearly one year of several measured wind conditions were considered for selection of loads and performance simulations. A new methodology for adjusting strain gauge (SG) calibrations originally from blade pull testing over time is presented. As a result, we show and discuss the different predictions on power performance and compare results with measured blade loads, under the condition of adjusting blade SG pull test calibration for temperature and time degradation effects.

1. Introduction

This paper presents a load validation between simulated loads using the aeroelastic code HAWC2 [1,2,3] and measured loads on an 850kW, 52 m diameter horizontal-axis VESTAS Wind Turbine [4]. The control of electrical power is performed using microprocessor-based monitoring of all turbine functions including OptiSpeed® rpm regulation and OptiTip® pitch regulation of the blades. The 44 m hub height wind turbine, see Figure 1 is located at DTU, Campus Risø, Denmark (UTM coordinate 317548183E, 6174985.312N). The mostly westerly winds at the fjord are orographic highly influenced to the left and right of the turbine by a strip of land characterized by higher roughness, and towards the open fjord the wind turbine experiences low turbulence winds. The mapped wind conditions for the V52 site are unpublished but comparable to the detailed inflow study [5] of a 500 kW wind turbine 180 m next to V52. Simulation results are here compared with measurements over several months of wind turbine operation. The studies covers seasonal effects with meteorological instruments, strain gauge (SG) measurements of blade loads as well as operational parameters such as rotor speed, pitch angle and electrical power. Furthermore, adjustment of SG calibration factors is presented based on low-wind speed idling where the turbine is in cut-in phase. This is different compared to static SG calibration, recommended in IEC practices [5], but was necessary in order to avoid drift in measurements. Results presented in this paper are based on the work of Gomiero during his 5 months Erasmus Mundus stay at DTU Wind Energy Department.

SG measurements are performed on the blade near the root. A list of signals determining the wind turbine conditions is shown in Table 1. Meteorological measurements are carried out at a 72m meteorological mast (metmast) placed 118m in front of the wind turbine towards West, with the measured wind speed at hub height. The metmast high-quality sensor installations comply with IEC61400-12[6] regarding



requirements for type, arm's length, orientation and distance/height of sensor. For an overview of metmast signals, see Figure 1. This paper i) explains the methodology for the validation practice; ii) shows simulation results obtained with the aero-elastic model and gives comparison with measurements focusing on blade load sensors calibration changes over time; finally iii) compares the results from the aero-elastic dynamic model with measured flap and edgewise blade bending moments. Fatigue loads are also considered in this paper.

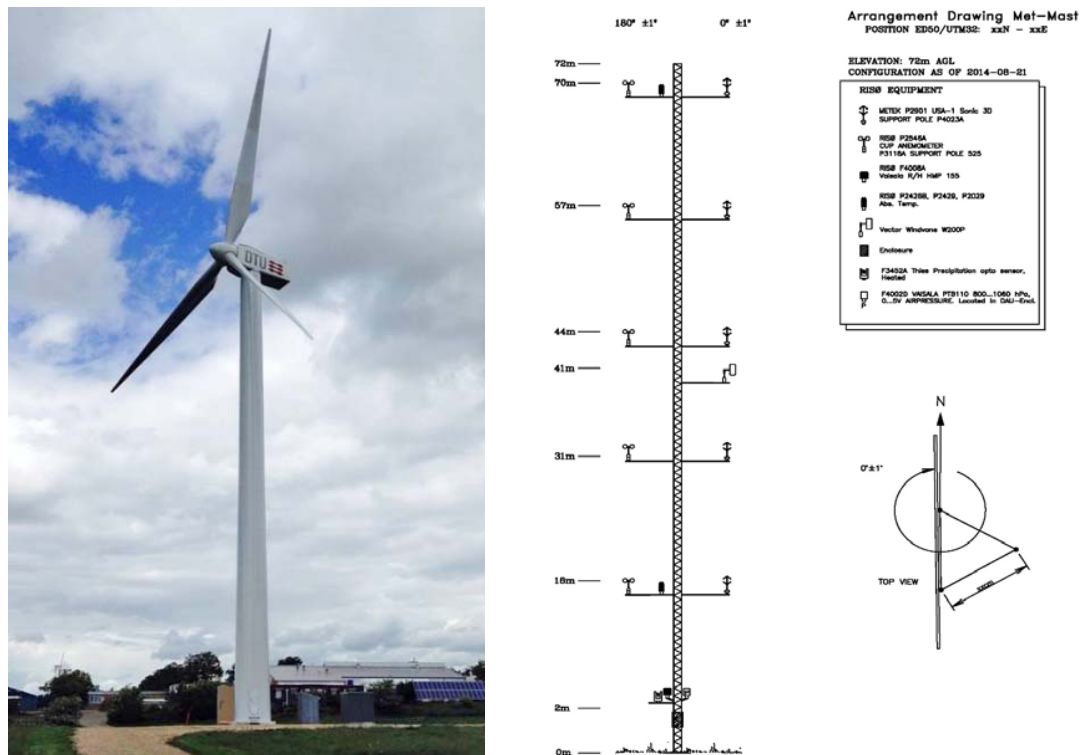


Figure 1: (Left) Photo of V52 at DTU campus Risø, from <http://www.powercurve.dk/our-technology> accessed on Nov 2017. (Right) Overview of installed sensors on the meteorological mast 2.5 diameters in front of the V52 wind turbine.

Table 1 Diagram of turbine sensors, VDF (Vestas Data Format) denotes an originally installed sensor while DTU denotes an additional sensor installed by DTU.

Signal	Unit	Type	Notes
Pitch	deg	VDF	Collective pitch angle
Rotor speed	rpm	VDF/DTU	RPM sensor
Azimuth	deg	DTU	Blade A position
El. Power	kW	VDF/DTU	Net available power
MxA	mV/V	DTU	Blade A root flapwise SGs
MyA	mV/V	DTU	Blade A root edgewise SGs
Nacelle wind speed	m/s	VDF	Sonic anemometer
Nacelle Yaw	deg	DTU	Nacelle position

2. Validation methodology

The validation approach is based on data collected during the test period under varying weather conditions. Instead of using the average sector wind characteristics a Monte-Carlo approach is used where simulations have been carried out for the exact same variations of wind speed, turbulence intensity (TI) and shear. The measurements and selection of data follows the IEC recommendations [5,6]. The overview of the data selection process and validation scheme is shown in Figure 2.

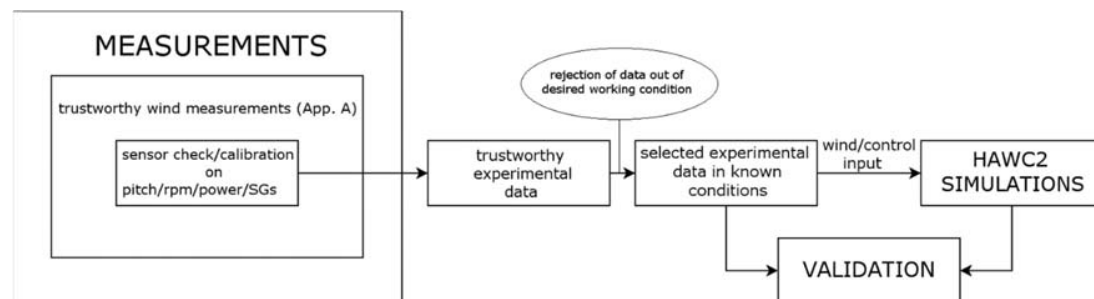


Figure 2: Schematics for process on selecting data and on validation

The method can be generally applied on wind turbines with pitch control. Figure 2 visualizes that site- and meteorological conditions were analysed for application of IEC 61400-12. In order to ensure that pitch, rpm and electrical power signals are measured correctly, all related sensor have been checked. Problems with these signals will erratically influence the emulation of the V52 controller. As an example, erratic simulated power curve conditions were experienced with the uncalibrated blade pitch system used as HAWC2 controller input. The blade pitch sensor calibration was made by correlating blade pitch position encoder signal and the physical angle obtained from a series of photos taken with locked rotor position at low wind conditions. These optical measurements of blade pitch angles were carried out over the full wind turbine operational range. Figure 3 shows that, depending on the control range of interest, errors (i.e. difference between sensor output and photo measured angle) appeared with different levels and are higher at pitch start and at pitch stop.

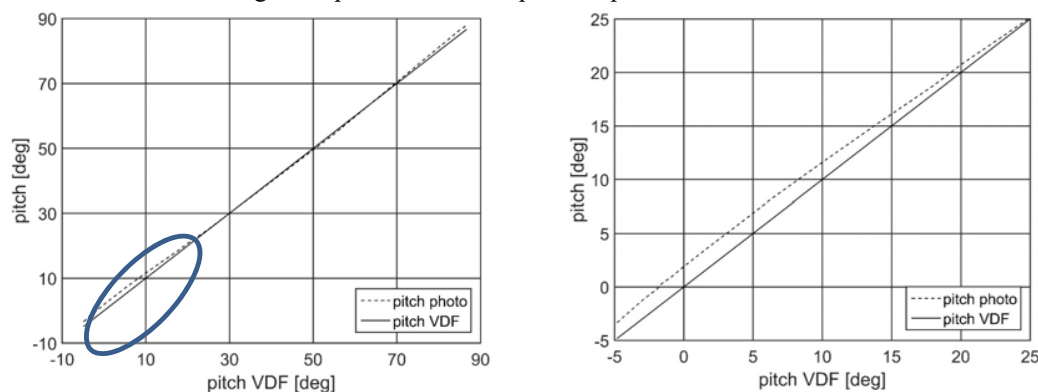


Figure 3: Pitch indication error. Left: operational range. Right: Enlarged area -5-25 Deg

Another important quality is reliable bending load signals. In Table 1 it is shown that blade root bending loads are measured with SGs in terms of mV/V^1 . In order to obtain the kNm measurement a linear dependency must be considered. The gain and offset constants were originally derived from a static blade pull test. Unfortunately SGs properties are influenced by temperature changes and degradation phenomena, and so is their output if constant calibration factors are used. In order to minimize

temperature and other gauge influences on measurements we adopted a scheme where SG output was analysed from periodic idling sequences, for including temperature and time changes in the initial calibration results. The deterministic bending moment cycles varies with the position of the blade mass centre during low speed idling, and this signal is used as a reference for SG calibration factors value adjustment. Figure 4 shows the calculated variation of gain and offset as a function of time and varying temperature for flapwise SG calibration factors. Using these curves, every SG output value¹ can be converted to bending load value [kNm] using different gain and offset based on the recorded temperature and date. This data selection and correction methodology generates data that defines the input conditions for simulating loads and performance of the wind turbine. Furthermore the data represents a measured and checked dataset that as indicated in Figure 2 is used for validation.

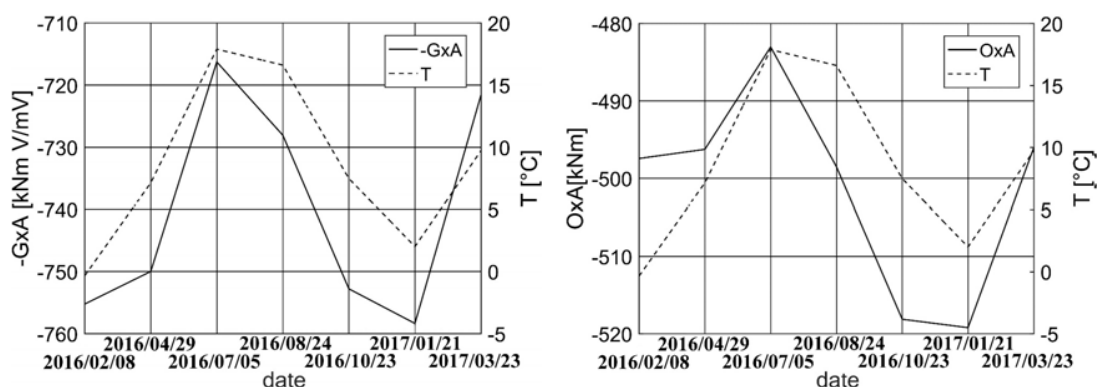
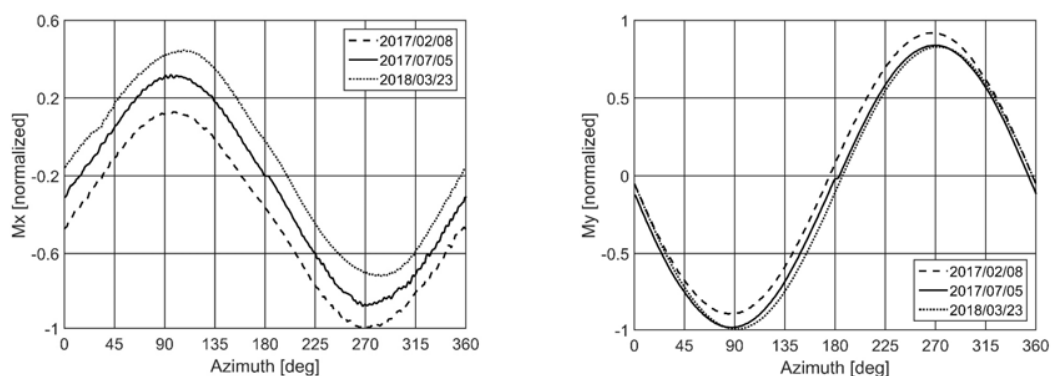


Figure 4: Flapwise SG calibration gain (G_{xA}) and offset values (O_{xA}) calculated during test period with different temperature (T , dashed) conditions.

As an example of using the rotor as a calibrating reference, graphs of idling sequences at three different occasions with low wind are shown in Figure 5. The upper graphs are derived using constant calibration factors as obtained from initial pull test, and the lower graphs are obtained with adjusted calibration factors. There is a clear tendency that the adjustment procedure guaranties a closer fit of the curves.



¹ The strain gauge amplifier output is in mV/V

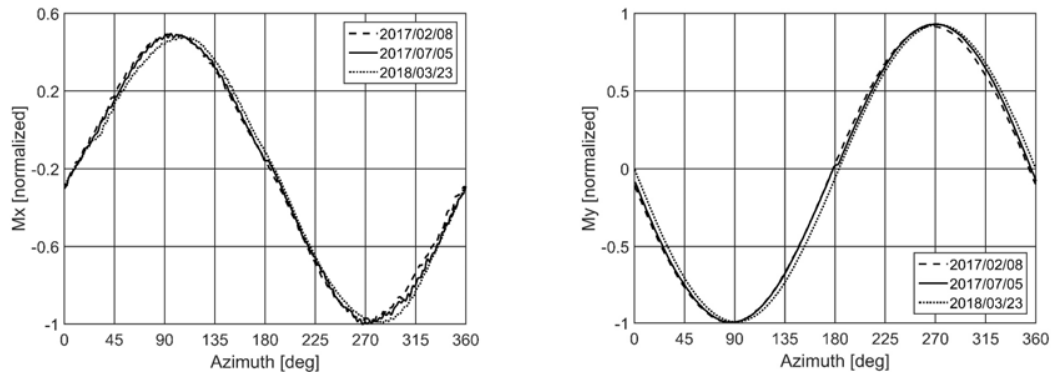
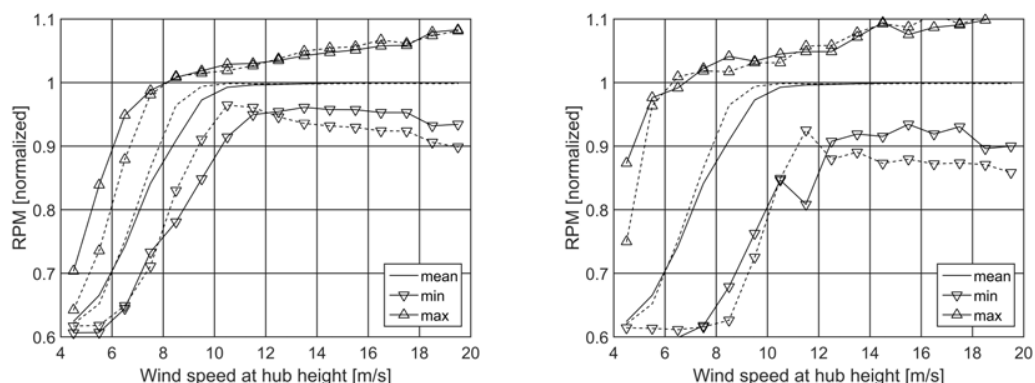


Figure 5: Top: Rotor idling sequence without and Bottom: with compensation of calibration factors

3. Aero-elastic simulations of wind turbine loads

Using analysed site - and meteorological conditions following IEC 61400-12 to define the inflow conditions, the aero-elastic solver predictions were compared on i) the prediction of power curve statistics and ii) load measurements statistics. In the simulations the BasicDTUController was used since the actual V52 controller was not available. No additional tuning of the controller parameters was done except to proper input for the controller, based on corrected rpm and pitch measurements was performed in order to ensure actual V52 behaviour is represented within a certain degree of confidence. The BasicDTUController theory and application is described in detail in [7] with source code and update manual². BasicDTUController is applicable for pitch-regulated, variable speed wind turbines. The calibrated pitch readout, rpm and power meter signal appears as input and filtered for the PIDs.

To demonstrate the controller output from measurements and from simulations, the following figures show statistics obtained for the rpm and pitch signals. The curves, see Figure 6 are average binned curves for maximum, minimum and mean values for simulated and measured data, and consider also the statistics of extremes. The comparison between measurements and simulations shows satisfactory agreement. Differences are likely attributed to non-linearity of the pitch actuator and likely the rpm feedback from the controller. At low wind speeds the simulated pitch excursion seems to deviate from actual measurements. However these sources were for this study not investigated in further details.



² source code:

<https://github.com/DTUWindEnergy/BasicDTUController/>

updated theory report:

<https://github.com/DTUWindEnergy/BasicDTUControllerReport>

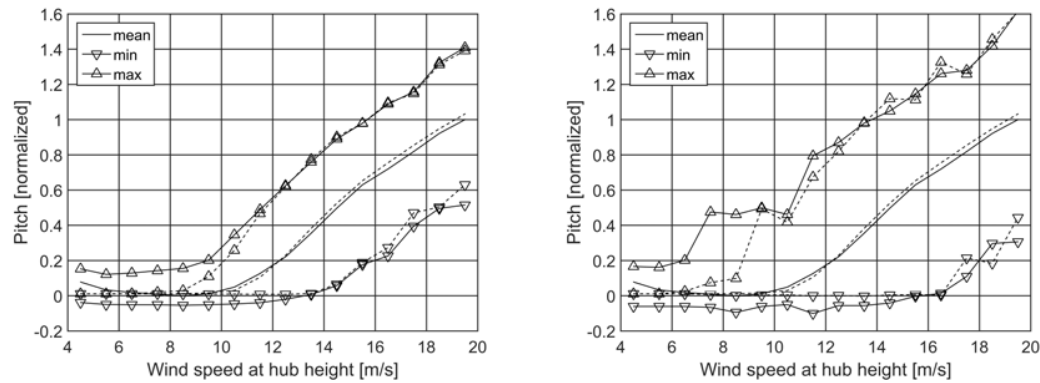


Figure 6: Controller output obtained from measurements (full line) and from simulations (dashed) with bin averages of mean, minimum and maximum, and bin averages of max of maxima, min of minima, and averages of means. Top: Rpm statistics. Bottom: Pitch statistics

Figure 7 compares bin-averaged statistics from measurements and simulations (dashed). HAWC2 predicts the mean binned power curve with a maximum relative error of 2.1%, compared to measured data.

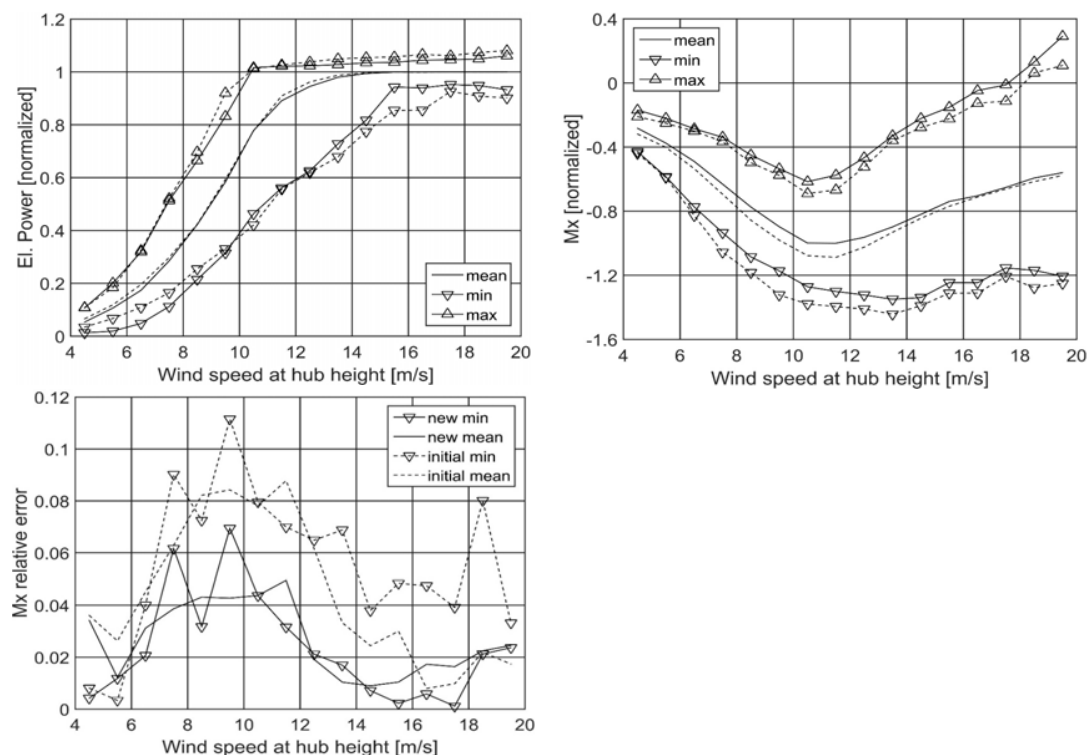


Figure 7: (Top Left): Statistics comparison for power curve and (Top Right): flap bending load M_x using pull test calibration factors. (Bottom Left): Relative error between simulated and measured bin-averaged M_x curves: initial calibration factors vs new factors.

Considering bending loads, as a first step the flapwise bending load M_x is calculated and plotted using the constant pull test calibration factors. In order to quantify the temperature/time corrected calibration

factors effect, relative error on M_x is shown for both constant and corrected calibration factors. This relative error is calculated by dividing the absolute difference between simulated and measured M_x bin-averaged curves by the peak value of the corresponding measured M_x bin-averaged curve. These peaks are found in the 11-12 m/s bin for mean curve and 13-14 m/s bin for min curve. When pull test calibration factors are used, M_x mean curve peak of the binned data is predicted with a maximum error below 9%. The average of local mins load curve error goes slightly above 11%. Both predictions are heavily enhanced by taking into account time/temperature SGs sensitivity, with almost halved relative error peak values, now below 5% and 7% respectively. Model fatigue loads prediction capability has been analysed for the MLC 1.1[8] capture matrix. Since temperature/time corrected strain gauge calibration coefficients are expected to reduce measurement uncertainties, they were applied in the following analysis for measured loads calculation. Rain flow counting following ASTM E1049-85[9] was applied to each 10 minutes time series M_x and M_y bending load signal from HAWC2 and from measurements in order to obtain the cumulative fatigue spectrum. In addition, 1 Hz Damage Equivalent Load (DEL) was calculated for each time series and its mean value was binned over wind speed. Regarding M_x cumulative spectrum, good agreement of number of cycles is observed between HAWC2 and measured data for significant load ranges. Maximum relative error registered between measurements and simulations on the M_x 1 Hz DEL curve is 8.6%. Regarding M_y fatigue spectrum, a significant difference between measured and simulated cycles was found below the global spectral peak in the range 20-200 kNm, shown in Figure 8. Since this peak is related to edgewise loads (determined by circular motion of a beam with distributed mass in a gravity field) and is well described, focus was attended to correct the M_y spectrum for misfits. Three probable causes for influencing the edgewise simulated bending moment were investigated: the structural model, the controller and the wind model.

The most plausible source for large differences were caused by misfit of the wind model. The standard practise of fitting the measured wind spectrum peak with a synthesised spectrum follows the recommended practice given in IEC 61400-1[10] and it follows the synthesis of the Mann model that neutral conditions are well described with adjusted length scale L and non-dimensional shear distortion parameter γ (IEC 61400-1 standard says standard value 3.9 for neutral conditions). However for the current validation a different method was tried out by adopting the following hypothesis: wind variations create blade loads and - deformations below the gravity peak range and it would be possible to see this effect with applying rain flow counting of the wind signal. If deformations and loads excursions are effects of turbulent wind, effects of this would be visible by applying load cycle analysis. The usual way to analyse mechanical loads follows the rain flow counting procedure. This unconventional use of the procedure is tested for comparison of simulated equivalent loads with measured equivalent loads M_y , and to use this comparison as a measure of how well the estimates fit to the measured equivalent load.

By trial and error we could see the match between simulations and measurements when changing the meteorological length scale L (standard value 25 m) and γ in the simulation results. Only for the length scale L significant effects on the fatigue spectrum were observed. The different graphs are shown in Figure 9 (left) illustrating the range of curves obtained for different L values. The $L = 55$ m spectrum was chosen as it is the nearest to the measured spectrum.

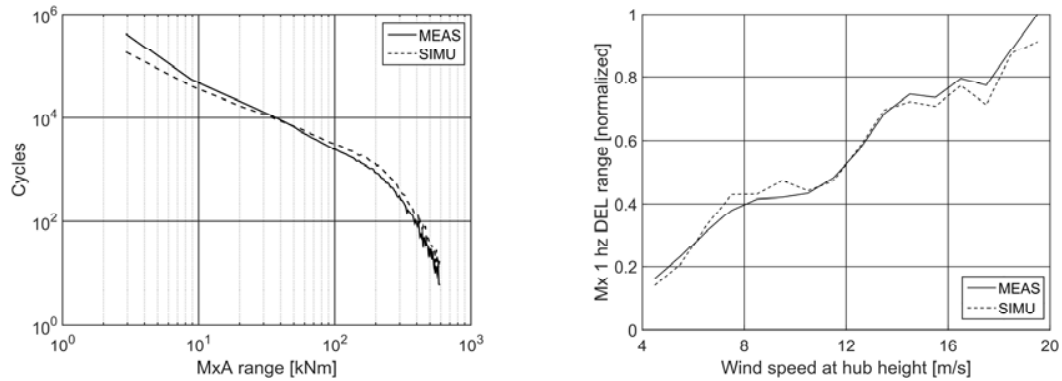


Figure 8: Comparison between simulated and measured data of flapwise bending moment load ranges (Left) and between simulated and measured 1 Hz DEL of flapwise bending moment (Right)

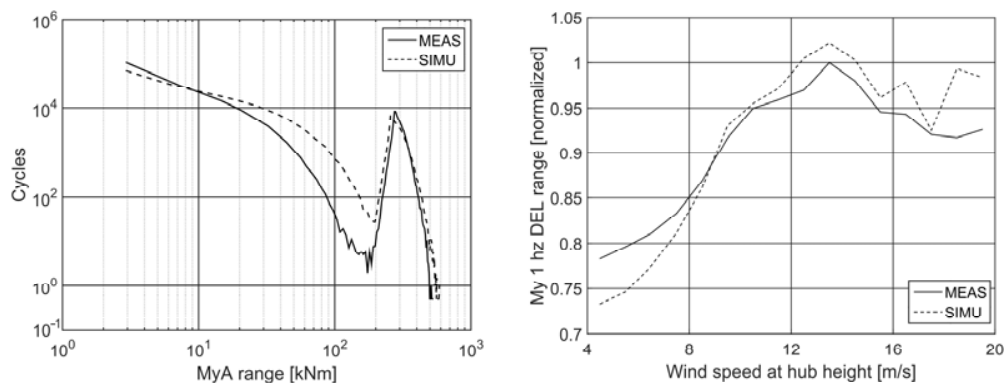


Figure 9: Comparison between simulated and measured data of edgewise bending moment load ranges (Left) and between simulated and measured 1 Hz DEL of edgewise bending moment (Right)

With this length scale value also the M_y 1 Hz DEL simulated curve is now in good qualitative agreement with measurements as shown in Figure 9 (Right), while in Figure 8 (standard L) the two curves were intersecting and DEL was over-predicted at high wind speeds. As expected, increasing the length scale decreased M_y cumulative fatigue cycles and this also decreased the M_y equivalent load, in particular at high wind speeds. Different γ values between 2.7 and 5 did not significantly change the M_x fatigue spectra, so that $\gamma=3.9$ was chosen as representative value. These results suggest that the L length scale value proposed by the standard is a safe-side assumption, and the method could be an intuitive way of achieving results obtained by extrapolating the length scale L from the actual measured wind spectrums for each time series. For a more detailed discussion on the validity of L and γ , the reader should consult a recent paper on the synthesis of conducting wind measurements for spectral characterisation [11]. For the present approach however, the results show, that the measured and the simulated equivalent loads estimation are deviating 2-6% (~ 20 kNm), with largest difference at low wind speeds. In the high wind speed range the differences tend to offset the M_y variations. The curves are identical allowing for variations within \pm one standard deviation.

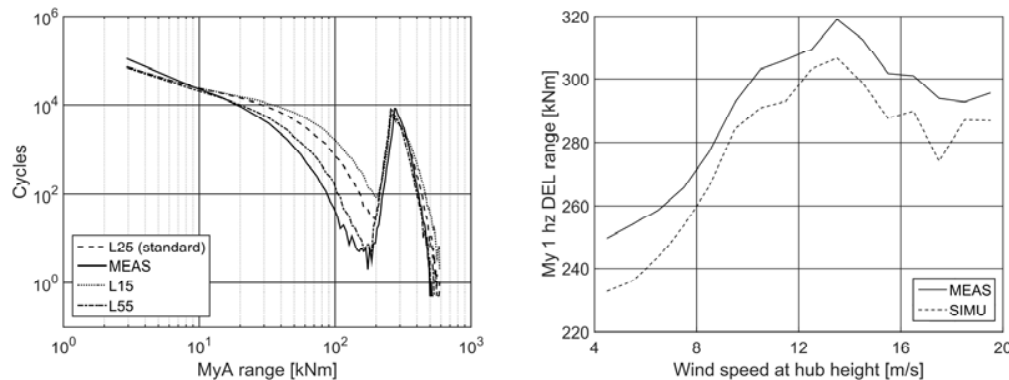


Figure 10: Left: Comparison between simulated and measured data of edgewise bending moment load ranges for different length scale L (15m, 25m, 55m). Right: comparison between simulated and measured edgewise bending moment for $L = 55$ m

Conclusions

An indirect validation of the V52 has been carried out with HAWC2 using an aero-elastic-servo model and verified data from wind turbine and metmast. For bending load binned curves the deviations between measurements and simulations are below 5% and improved to past results of 10%. The controller model adopted with a linear calibration model of the pitch system, validated rpm and power transducer provides a power curve mostly identical to the measured power curve. Differences are attributed to the non-linear static pitch calibration curve. The wind model spectrum has been fitted by finding a best fit of the meteorological length scale L with focus to particularly decrease the errors between measured and simulated equivalent load spectrum as low as 2-6%. It is also noted that better results could be obtained computing the actual length scale from each measured wind signal. The method demonstrates that the errors between measured and simulated loads are reduced from roughly 10% to 2-6%.

Acknowledgement

VESTAS is kindly acknowledged for their support in providing data of the wind turbine. DTU Wind Energy Department and Padua University is thanked for supporting this work.

References

- [1] Larsen T J and Hansen A M 2015 How 2 HAWC2, the user's Manual Risø-R-1597(ver4-6)(EN)
- [2] Larsen T J, Aagaard Madsen H, Larsen G C and Hansen K S 2013 Validation of the dynamic wake meander model for loads and power production in the Egmond aan Zee wind farm
- [3] Koukoura C, Natarajan A and Branner K. 2014 Validated Loads Prediction Models for Offshore Wind Turbines for Enhanced Component Reliability
- [4] VESTAS company product info:V52-850kW the Turbine that goes anywhere.
<http://www.vestas.cz/files/V52-850.pdf>, accessed Nov 2017
- [5] Paulsen U S and Wagner R 2012 IMPER: Characterization of the Wind Field over a Large Wind Turbine Rotor : Final report. 335 p. (DTU Wind Energy E; No. 0002).
- [6] IEC61400-12 2017 Power performance measurements of electricity producing wind turbines
- [7] Hansen M H, Henriksen L C Basic DTU Wind Energy controller. DTU Wind Energy, 2013. 43 p. (DTU Wind Energy E; No. 0028).
- [8] IEC61400-13 2015 Measurement of mechanical loads
- [9] ASTM E1049-85 2017 Standard Practices for Cycle Counting in Fatigue Analysis

- [10] IEC61400-1 2005 Wind turbines-part 1: Design requirements
- [11] Kelly M 2018 From standard wind measurements to spectral characterization: turbulence length scale and distribution <https://doi.org/10.5194/wes-2018-14>